C. R. Mecanique 342 (2014) 485–489

Contents lists available at ScienceDirect

Comptes Rendus Mecanique

www.sciencedirect.com

Relative periodic orbits in plane Poiseuille flow

Subhendu Rawat [a], Carlo Cossu [a,*], François Rincon [b,c]

[a] Institut de mécanique des fluides de Toulouse, CNRS and Université de Toulouse, allée du Professeur-Camille-Soula, 31400 Toulouse, France
[b] Université de Toulouse, UPS–OMP, IRAP, Toulouse, France
[c] CNRS, IRAP, 14, avenue Édouard-Belin, 31400 Toulouse, France

ARTICLE INFO

Article history:
Received 23 March 2014
Accepted 23 May 2014
Available online 25 June 2014

Keywords:
Fluid dynamics
Hydrodynamic stability
Transition to turbulence

ABSTRACT

A branch of relative periodic orbits is found in plane Poiseuille flow in a periodic domain at Reynolds numbers ranging from $Re = 3000$ to $Re = 5000$. These solutions consist in sinuous quasi-streamwise streaks periodically forced by quasi-streamwise vortices in a self-sustained process. The streaks and the vortices are located in the bulk of the flow. Only the amplitude, but not the shape, of the averaged velocity components does change as the Reynolds number is increased from 3000 to 5000. We conjecture that these solutions could therefore be related to large- and very large-scale structures observed in the bulk of fully developed turbulent channel flows.

1. Introduction

Transition to turbulence is subcritical in most canonical internal flows, such as the pressure-driven plane channel and pipe flows, or the plane Couette flow. To gain insight into the transition process, a fruitful approach has been to apply the nonlinear dynamical systems methodology to analyze the dynamics of the flow in small horizontally periodic domains. Following this approach, the subcritical transition to turbulence, is correlated with the appearance of additional solutions of the Navier–Stokes equations disconnected from the laminar solution. Nonlinear traveling waves (NTW), representing saddles in phase space, have been shown to appear at Reynolds numbers much lower than the transitional ones in plane Couette flow [24,3,29], plane channel flow [9,30], and pipe flow [10,31]. It was initially believed that turbulent solutions may spend a significant time in the neighborhood of relevant NTW, but it was later shown that these visits last only 10–20%, on average, of the total time [19,26]. Attention has therefore shifted to unstable periodic (in time) solutions (periodic orbits or relative periodic orbits), both for their potentially very important role in the transition process and because they might provide the missing building blocks to predict the statistics of the chaotic attractor or repeller itself [1]. Periodic solutions have been computed in plane Couette [4,18,28], plane channel [27] and pipe flows [7], as well as in the asymptotic suction boundary layer [22]. The confirmation that unstable periodic orbits and their stable and unstable manifolds are associated with transition to chaos in small spatially periodic domains has been recently given in plane Couette flow [23] and in magnetohydrodynamic Keplerian shear flows [25].

Nonlinear traveling waves and periodic solutions show an interplay between quasi-streamwise streaks and vortices that is also characteristic of the turbulent dynamics. This self-sustained process is believed to explain the dynamics in the near-wall region of turbulent flows [13,8], and self-sustained processes at larger scales [15,16], which are important at large Reynolds numbers (see, e.g., [21,20,12]).

* Corresponding author.

http://dx.doi.org/10.1016/j.crme.2014.05.008
1631-0721/

In this study, we consider the existence of periodic solutions in the plane channel flow, which is less investigated than plane Couette and pipe flows, despite its intrinsic interest and its dynamic similarity with boundary layer flows which are of interest to industrial applications. In the case of plane Poiseuille flow at $Re = 3000$ in a periodic domain of streamwise and spanwise size $L_x = \pi h$ and $L_z = 0.4\pi h$, an NTW solution was first found [17] using a bisection procedure that started with an initial guess based on a turbulent solution. A later study in the same domain at the same Re, but using different initial conditions in the bisection procedure, revealed the existence of a "periodic-like solution" [27], i.e. a solution that could be either a genuine periodic solution or a heteroclinic connection (a single period of the solution was accessible due to numerical precision issues). Both solutions were localized on a single wall of the channel and are therefore thought to evolve to near-wall structures for increasing Reynolds numbers. In the current state of affairs, however, no solution that may be correlated with the large-scale dynamics of detached eddies in the bulk of the flow is available. The scope of the present investigation is therefore to find if periodic solutions related to large-scale structures in fully developed turbulent flows exist with amplitudes that remain finite in the whole channel.

After a summary of the problem formulation and of the techniques used to isolate periodic solutions in plane channel flow in Section 2, the main properties of the relative periodic orbits discovered are described in Section 3. The results are finally briefly discussed in Section 4.

2. Problem formulation and methods

We consider the pressure-gradient-driven flow of an incompressible viscous fluid of constant density ρ and kinematic viscosity ν in a plane channel of height $2h$. The flow is ruled by the Navier–Stokes equations, which in dimensionless form, read:

$$\nabla \cdot \mathbf{u} = 0 \tag{1}$$

$$\frac{\partial \mathbf{u}}{\partial t} + \mathbf{u} \cdot \nabla \mathbf{u} = -\nabla p + \frac{1}{Re} \nabla^2 \mathbf{u} \tag{2}$$

where the Reynolds number $Re = U_0 h/\nu$ is defined with respect to the maximum velocity U_0 of the usual laminar (parabolic) Poiseuille solution. Velocities are made dimensionless with respect to U_0, pressures with respect to ρU_0^2, lengths with respect to h and times with respect to h/U_0. We denote by x the streamwise axis aligned with the pressure gradient, by y and z the wall-normal and spanwise coordinates and by u, v and w the velocity components along x, y and z, respectively. The flow is solved inside the domain $[0, L_x] \times [-1, 1] \times [0, L_z]$, with no-slip conditions on both walls and periodic boundary conditions is the streamwise and spanwise directions.

In order to find periodic solutions that do not migrate to the near wall-region for increasing Reynolds numbers, we found it useful to enforce the mid-plane reflection symmetry $\{u, v, w\}(x, y, z) = \{u, -v, w\}(x, -y, z)$. A standard bisection procedure on the initial conditions was used to track the edge state solutions within the enforced symmetry class. The initial conditions considered consist in the laminar Poiseuille solution perturbed by a pair of streamwise uniform counter-rotating vortices of amplitude A_1 and a sinuous perturbation of the spanwise velocity with amplitude A_2:

$$\mathbf{u}_0 = \{U_{\text{lam}}(y), 0, 0\} + A_1 \left\{0, \frac{\partial \psi_0}{\partial z}, -\frac{\partial \psi_0}{\partial y}\right\} + A_2 \{0, 0, w_{\sin}\} \tag{3}$$

where

$$\psi_0(y, z) = \left(1 - y^2\right) \sin(\pi y) \sin\left(\frac{2\pi z}{L_z}\right); \qquad w_{\sin}(x, y) = \left(1 - y^2\right) \sin\left(\frac{2\pi x}{L_x}\right) \tag{4}$$

The stream function $\psi_0(y, z)$ is associated with streamwise uniform vortices, while $w_{\sin}$ provides the (streamwise) sinuous perturbation. The initial velocity fields $\mathbf{u}_0$ are solenoidal and have the same volume flux as the laminar Poiseuille solution $U_{\text{lam}} = 1 - y^2$. The bisection is operated on A_1 with the ratio $A_2/A_1 = 1/10$ kept fixed to a relatively small value allowing the subcritical development of the streak instability [5,6].

The Navier–Stokes equations are integrated using the `channelflow` code [11], which is based on a Fourier–Chebyshev–Fourier spatial pseudospectral discretization. Solutions are advanced in time using a second-order Crank–Nicolson Runge–Kutta time stepping. Typically, results were obtained with $16 \times 41 \times 16$ points in the streamwise, wall-normal, and spanwise directions, and enforcing a constant volume flux during the simulation. We verified that the characteristics of the periodic solutions found by bisection on the coarse grid do not change when the number of collocation points is increased to $32 \times 65 \times 32$. The numerical results were further tested by recomputing the same periodic solutions with the different code `diablo` [2]. The convergence of the periodic solutions was validated and improved using Newton-based iterative methods and then their linear stability was analyzed using the `peanuts` code [14,25].

3. Results

We consider the domain of extension $2\pi \times 2 \times 2.416$, for which the nonlinear traveling waves solutions appear at the lowest Reynolds number [30], and Reynolds numbers ranging from $Re = 3000$ to 5000. For all these Reynolds numbers,

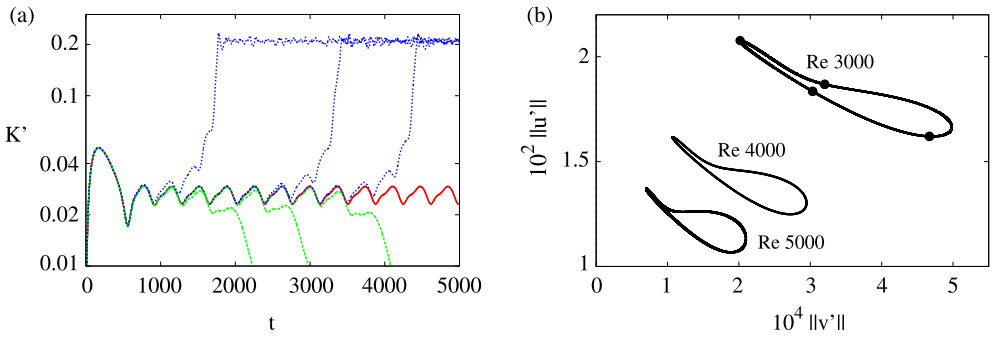

Fig. 1. (Color online.) Panel (a): Temporal dependence of the perturbation kinetic energy for selected iterations of the bisection process at $Re = 3000$. The solution on the edge rapidly converges to a periodic solution. Panel (b): Converged periodic solutions represented in the $\|v'\|$–$\|u'\|$ plane for $Re = 3000$, 4000, and 5000.

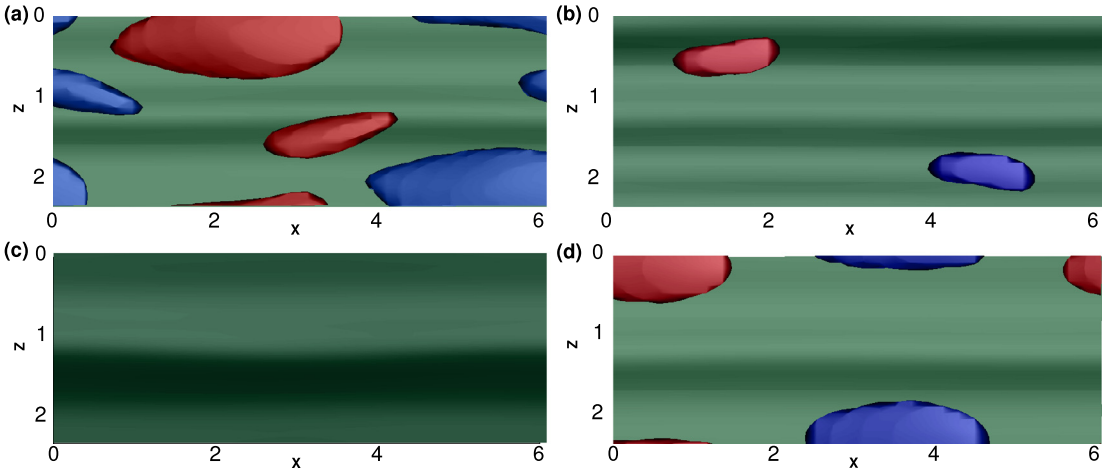

Fig. 2. (Color online.) Snapshots of the converged periodic solution obtained at $Re = 3000$. Four snapshots are taken in correspondence to the points reported on the cycle in Fig. 1b starting from the bottom left point and then rotating counterclockwise. The snapshots are taken at respectively $t = 0$ (panel (a)), $t = 120$ (panel (b)), $t = 230$ (panel (c)) and $t = 310$ (panel (d)). Only the top half of the channel is considered. The figure displays the iso-levels of the perturbation streamwise velocity field taken at $y = h/2$ are reported. In green is reported the surface where the streamwise velocity is 75% of its maximum value in the whole channel. In respectively blue and red are reported the surfaces where the streamwise vorticity is ±60% of its maximum value in panel (a) with the same value in all panels. In particular, no vortices are visible in panel (c), because they are of very low amplitude.

the laminar Poiseuille solution is linearly stable, while perturbations with sufficiently large amplitude lead to a turbulent state. Solutions living on the boundary of the basin of attraction of the laminar state are found by applying the bisection procedure described in Section 2. The bisection looks for the threshold A_1 corresponding to the basin boundary. Values of A_1 slightly above the threshold lead to turbulent solutions (dashed, blue lines in Fig. 1a), while values slightly below lead to the laminar state (dotted, green lines in Fig. 1a). For sufficiently long times and for values of A_1 that are sufficiently good approximations of the exact threshold, the solutions on the basin boundary converge to a relative periodic orbit for all cases considered (see Fig. 1a for the $Re = 3000$ convergence) with a period that increases with the Reynolds number ($T = 739$ for $Re = 3000$, $T = 1090$ for $Re = 4000$ and $T = 1418$ for $Re = 5000$). The periodic solutions are found to travel in the streamwise direction with a phase speed $C_x = 0.98$ for $Re = 3000$ and 0.985 for the two other cases. This indicates that the active part of the process is located near the channel center. In Fig. 1b, the converged periodic solutions are shown in the $\|v'\|$–$\|u'\|$ plane, where $\|u'\|^2 = (1/\mathcal{V}) \int_{\mathcal{V}} (u - U_{\text{lam}})^2 \mathrm{d}\mathcal{V}$ and $\|v'\|^2 = (1/\mathcal{V}) \int_{\mathcal{V}} v^2 \mathrm{d}\mathcal{V}$. The norm $\|u'\|$ of the streamwise perturbation velocity is representative of the amplitude of streamwise streaks, while $\|v'\|$ is representative of the amplitude of the quasi-streamwise vortices. The solutions rotate counter-clockwise in the cycles reported in Fig. 1b. Starting from a point on the bottom-right of the cycle, where the amplitude of the vortices is maximum, the amplitude of the vortices initially decays while that of the streaks increases, due to the lift-up mechanism. The streaks then reach a maximum amplitude where they experience a breakdown during which their amplitude decays fast, while regenerating the vortices, which closes the loop of the classical self-sustained process [13]. The solution travels quite fast in the lower part of the cycle, as can be seen also in Fig. 1a, where it is seen that the growth phase (lift-up) of $K' \approx \|u'\|^2$ is much slower than the decay phase (breakdown). The evolution of the flow structures during the cycle can be seen in the snapshots of the flow field displayed in Fig. 2, taken in correspondence to the four points shown in Fig. 1b. The converged periodic solutions have the shift and reflect symmetry $\{u, v, w\}(x, y, z) = \{u, v, -w\}(x + Lx/2, y, -z)$, which was not enforced on the initial

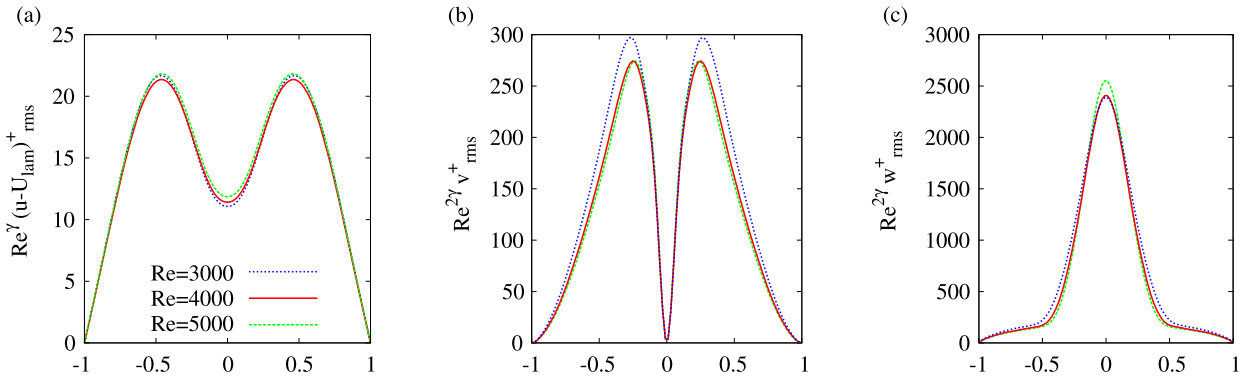

Fig. 3. (Color online.) Rescaled *rms* amplitudes of the periodic velocity perturbations expressed in wall units and averaged over one period. The streamwise, wall-normal and spanwise components are reported in panels (a), (b) and (c), respectively. The solutions are rescaled using the value $\gamma = 0.8$.

Table 1
Real parts σ_j of the j-th Floquet exponents of the unstable modes of the periodic orbit solutions.

Re	$10^3\sigma_1$	$10^3\sigma_2$	$10^3\sigma_3$	$10^3\sigma_4$	$10^3\sigma_5$
3000	3.99	3.34	3.32	2.99	2.73
4000	3.39	1.34	1.16	1.06	1.03

condition. From the snapshots it is seen how every half-period the low speed streak and the quasi-streamwise vortices shift by half spanwise wavelength and then repeat the cycle exactly in the same way due to the shift and reflect the symmetry of the solutions. One period therefore corresponds to two loops of the cycles reported in Fig. 1b.

From Fig. 1b we see that the amplitude of the relative periodic solutions decreases for increasing Reynolds numbers, which is typical of 'lower branch' solutions that live on the edge of chaos (see, e.g., [23] for the asymptotic suction boundary layer case). An examination of the root-mean-square velocity field perturbation, averaged over the horizontal planes and one temporal period, shows that most of the perturbation *rms* kinetic energy resides in the streamwise velocity component (streaks) with a maximum amplitude located near $y \approx \pm 1/2$. The wall-normal and spanwise velocity *rms* profiles are consistent with center-channel quasi-streamwise vortices. These periodic solutions, therefore, unlike previously found periodic-like solutions [27], are not localized near a single wall, but in the bulk of the flow.

When the Reynolds number is increased, the *rms* amplitude of the velocity field perturbation is seen to decrease. The velocity *rms* profiles remain approximately self-similar, with amplitudes decreasing as $Re^{-\gamma}$ for the streamwise velocity and $Re^{-2\gamma}$ for the wall-normal and the spanwise velocity components, with $\gamma \approx 0.8$. The facts that the streaks amplitude is always larger than the vortices amplitude and that the ratio of streak to vortices amplitudes is almost proportional to the Reynolds number are additional indications that the non-normal amplification of streaks from the vortices plays an important role in the self-sustainment of these periodic solutions (Fig. 3).

These periodic solutions are unstable. A Floquet linear stability analysis was performed at $Re = 3000$ and 4000, once the convergence of the periodic solution was improved to sufficient accuracy using Newton iterations. If no symmetry is enforced, five unstable exponents are found, but only one mode (the most unstable) has the same symmetries of the periodic orbit solution. All the unstable Floquet exponents are real and their real part, reported in Table 1, decreases when the Reynolds number is increased.

4. Conclusions

Unstable periodic solutions of the Navier–Stokes equations have been computed in a minimal box for plane Poiseuille flow at Reynolds numbers ranging from $Re = 3000$ to $Re = 5000$. These solutions have long periods that increase with *Re* and that are of the order of a thousand convective time units. The averaged velocity field perturbations are approximately self-similar in *Re*, with different velocity components scaling differently with the Reynolds number. The self-similar velocity fields are associated with quasi-streamwise streaks and vortices located in the bulk of the flow. The streaky structures associated with the relative periodic orbits do not migrate to the near-wall region as the Reynolds number is increased. These structures, which remain situated in the bulk of the flow for increasing Reynolds numbers and which are associated with quite low frequencies of oscillation, are therefore compatible with large- and very large-scale structures whose role is crucial in turbulent flows at high Reynolds numbers. Two recent investigations indicate indeed that self-sustained processes exist at large- and very large-scale in the bulk of the flow [15] and in the logarithmic layer [16] of turbulent channel flows and that these processes are not forced by the near-wall cycle. It is therefore tempting to link the large scale self-sustained processes in the bulk of the flow to a 'backbone' of underlying periodic solutions, following the same rationale invoked for the near-wall structures. Current effort is aimed at providing evidence supporting this conjecture, namely by quantifying the

phase speeds of the large-scale structures, by computing their correlations to the found periodic solutions, and, even most importantly, by computing additional periodic solutions that might be of interest to this approach.

Acknowledgements

The use of the `channelflow.org` code [11] and financial support (grant no. 11050707) from PRES Université de Toulouse and Région Midi-Pyrénées are kindly acknowledged.

References

[1] R. Artuso, E. Aurell, P. Cvitanovic, Recycling of strange sets: I. Cycle expansions, Nonlinearity 3 (1990) 325.
[2] T.R. Bewley, Numerical Renaissance: Simulation, Optimization and Control, Renaissance Press, San Diego, CA, USA, 2008.
[3] R.M. Clever, F.H. Busse, Three-dimensional convection in a horizontal fluid layer subjected to a constant shear, J. Fluid Mech. 234 (1992) 511–527.
[4] R.M. Clever, F.H. Busse, Tertiary and quaternary solutions for plane Couette flow, J. Fluid Mech. 344 (1997) 137–153.
[5] C. Cossu, M. Chevalier, D.S. Henningson, Secondary optimal growth and subcritical transition in the plane Poiseuille flow, in: P. Schlatter, D.S. Henningson (Eds.), Seventh IUTAM Symposium on Laminar–Turbulent Transition, Springer, 2010, pp. 129–134.
[6] C. Cossu, L. Brandt, S. Bagheri, D.S. Henningson, Secondary threshold amplitudes for sinuous streak breakdown, Phys. Fluids 23 (2011) 074103.
[7] Y. Duguet, C.C.T. Pringle, R.R. Kerswell, Relative periodic orbits in transitional pipe flow, Phys. Fluids 20 (11) (2008) 114102.
[8] T. Duriez, J.-L. Aider, J.E. Wesfreid, Self-sustaining process through streak generation in a flat-plate boundary layer, Phys. Rev. Lett. 103 (2009) 144502.
[9] U. Ehrenstein, W. Koch, Three-dimensional wavelike equilibrium states in plane Poiseuille flow, J. Fluid Mech. 228 (1991) 111–148.
[10] H. Faisst, B. Eckhardt, Travelling waves in pipe flow, Phys. Rev. Lett. 91 (2003) 24502.
[11] J.F. Gibson, J. Halcrow, P. Cvitanovic, Visualizing the geometry of state space in plane Couette flow, J. Fluid Mech. 611 (2008) 107–130.
[12] M. Guala, S.E. Hommema, R.J. Adrian, Large-scale and very-large-scale motions in turbulent pipe flow, J. Fluid Mech. 554 (2006) 521–541.
[13] J.M. Hamilton, J. Kim, F. Waleffe, Regeneration mechanisms of near-wall turbulence structures, J. Fluid Mech. 287 (1995) 317–348.
[14] J. Herault, F. Rincon, C. Cossu, G. Lesur, G.I. Ogilvie, P.-Y. Longaretti, Periodic magnetorotational dynamo action as a prototype of nonlinear magnetic field generation in shear flows, Phys. Rev. E 84 (2011) 036321.
[15] Y. Hwang, C. Cossu, Self-sustained process at large scales in turbulent channel flow, Phys. Rev. Lett. 105 (4) (2010) 044505.
[16] Y. Hwang, C. Cossu, Self-sustained processes in the logarithmic layer of turbulent channel flows, Phys. Fluids 23 (2011) 061702.
[17] T. Itano, S. Toh, The dynamics of bursting process in wall turbulence, J. Phys. Soc. Jpn. 70 (2001) 703–716.
[18] G. Kawahara, S. Kida, Periodic motion embedded in plane Couette turbulence: regeneration cycle and burst, J. Fluid Mech. 449 (2001) 291–300.
[19] R.R. Kerswell, O.R. Tutty, Recurrence of traveling waves in transitional pipe flow, J. Fluid Mech. 584 (2007) 69–102.
[20] K.C. Kim, R. Adrian, Very large-scale motion in the outer layer, Phys. Fluids 11 (2) (1999) 417–422.
[21] L.S.G. Kovasznay, V. Kibens, R.F. Blackwelder, Large-scale motion in the intermittent region of a turbulent boundary layer, J. Fluid Mech. 41 (1970) 283–325.
[22] T. Kreilos, B. Eckhardt, Periodic orbits near onset of chaos in plane Couette flow, Chaos 22 (4) (2012) 047505.
[23] T. Kreilos, G. Veble, T.M. Schneider, B. Eckhardt, Edge states for the turbulence transition in the asymptotic suction boundary layer, J. Fluid Mech. 726 (2013) 100–122.
[24] M. Nagata, Three-dimensional finite-amplitude solutions in plane Couette flow: bifurcation from infinity, J. Fluid Mech. 217 (1990) 519–527.
[25] A. Riols, F. Rincon, C. Cossu, G. Lesur, P.-Y. Longaretti, G.I. Ogilvie, J. Herault, Global bifurcations to subcritical magnetorotational dynamo action in Keplerian shear flow, J. Fluid Mech. 731 (2013) 1–45.
[26] T.M. Schneider, B. Eckhardt, J. Vollmer, Statistical analysis of coherent structures in transitional pipe flow, Phys. Rev. E 75 (2007) 066313.
[27] S. Toh, T. Itano, A periodic-like solution in channel flow, J. Fluid Mech. 481 (2003) 67–76.
[28] D. Viswanath, The dynamics of transition to turbulence in plane couette flow, arXiv:physics/0701337, 2007.
[29] F. Waleffe, Three-dimensional coherent states in plane shear flows, Phys. Rev. Lett. 81 (1998) 4140–4143.
[30] F. Waleffe, Homotopy of exact coherent structures in plane shear flows, Phys. Fluids 15 (2003) 1517–1534.
[31] H. Wedin, R.R. Kerswell, Exact coherent structures in pipe flow: traveling wave solutions, J. Fluid Mech. 508 (2004) 333–371.